10.1098/rspa.2003.1223

THE ROYAL SOCIETY

A fast algorithm for the simulation of polycrystalline misfits. II. Martensitic transformations in three space dimensions

By Guillermo H. Goldsztein[1] and Oscar P. Bruno[2]

[1]*Georgia Institute of Technology, School of Mathematics, Atlanta, GA 30332, USA*
[2]*Applied and Computational Mathematics, Caltech, Pasadena, CA 91125, USA*
(ggold@math.gatech.edu)

Received 24 April 2003; accepted 11 August 2003; published online 9 March 2004

We present a fast numerical method for the simulation of martensitic transformations in three-dimensional polycrystals. To produce the relevant overall elastic energy arising from given boundary conditions, this method proceeds by reducing the corresponding non-convex minimization problem to minimization of a certain *quadratic form*—over the set of arrays of transformation strains which are compatible with a given distribution of crystallite orientations. The evaluation of this quadratic form for a given array of transformation strains requires solution of certain *linear* elasticity problems. An acceleration strategy we use, which for a polycrystal containing N grains reduces the complexity of the algorithm from $\mathcal{O}(N^2)$ to $\mathcal{O}(N)$ operations, results from a formulation of the minimization problem which takes advantage of certain decorrelations present in the minimizing arrays of transformation strains. We illustrate our presentation with a number of examples involving cubic-to-monoclinic and cubic-to-orthorhombic polycrystalline phase transitions, such as those arising in the TiNi and CuAl shape-memory alloys. In particular, our study quantifies the effects of texture on the overall properties of such polycrystalline shape-memory alloys.

Keywords: phase transformation; polycrystalline material; numerical algorithms; homogenization

1. Introduction

Martensitic transformations are solid-to-solid phase transitions that can be induced in certain crystalline materials as a result of changes in temperature or applied stresses. These phase transitions, one of whose microscopic manifestations is a change in the atomic spacings of the corresponding crystalline lattices, are associated with rather notorious macroscopic deformations (Wayman 1964; Wechsler *et al*. 1953). In this paper we consider martensitic transformations in polycrystalline solids.

Since, typically, the deformations associated with a phase transition in a single crystal are anisotropic, phase transitions in polycrystalline samples necessarily give rise to misfits between the transformation strains of neighbouring grains; clearly, such misfits play essential roles in polycrystalline phase transitions. To treat the (nonlinear) misfit problem we evaluate the relevant overall elastic energy by means of a fast

 © 2004 The Royal Society

three-dimensional algorithm. We apply our methods to a number of cases involving cubic-to-orthorhombic and cubic-to-monoclinic polycrystalline phase transitions, such as those arising in the CuAl and TiNi systems. We use our method to study the dependence of recoverable strains on the texture, i.e. the spatial distribution of orientations.

To evaluate the overall energy of martensitic polycrystals we appeal to the small-grain homogenization limit, which allows us to assume (i) spatially uniform crystal orientation statistics (texture), and (ii) homogeneous applied displacements. We then use the Green function associated with the equations of *linear elasticity* to obtain an explicit expression for the elastic energy as a function of the applied strain and the distribution of transformation strains. This expression, which is a quadratic function in the transformation strains, can be used to reduce the complete *nonlinear* minimization problem to a constrained minimization of a quadratic function in a large number of variables. This minimization is efficiently performed through a convergent sequence of approximations that reduce the complexity of the method from $O(N^2)$ to $O(N)$ operations, where N is the number of grains that make up the polycrystal.

In its present form our numerical method applies under some restrictions, as detailed in what follows. Firstly, the method assumes that the grains are firmly bonded, and that the phase transition does not result in plastic deformations or fracture either within the grains or along grain boundaries. In addition, it assumes that, under small deformations, both the martensite and the austenite are elastically isotropic, and that the two phases have identical elastic constants. Finally, it assumes that the transformation strain of each grain is *mesoscopically uniform* (as is indeed the case uniformly twinned grains and in small-grain polycrystals), and it neglects the rotations that arise as a result of phase transition (Wechsler *et al*. 1953).

While these restrictions are not good approximations for some systems, the resulting computations do provide insights on the behaviour of polycrystalline phase transitions. Further, all of these restrictions can be relaxed through suitable generalizations of our methods; the simpler, ideal case considered here should serve as a guide in the study of these complex systems, and in the development of more comprehensive simulations.

In §§ 4 *a*(iii) and 4 *b*(i) we introduce a criterion for recoverability of strains in martensitic polycrystals, which considers a strain recoverable if the associated overall energy does not exceed a certain value. This type of criterion has been considered by Bhattacharya & Kohn (1997). Using this criterion, we study with our numerical methods the dependence of the recoverable strain on the texture.

A version of our algorithm for two-dimensional polycrystals was introduced in Bruno & Goldsztein (1999). A preliminary version of the algorithm presented here was announced in Bruno & Goldsztein (2000). In this paper, we extend the algorithm presented in Bruno & Goldsztein (2000), which allows us to treat cubic-to-monoclinic phase transitions.

This paper is organized as follows. After describing our mathematical model in § 2, in § 3 we present our numerical method, and we demonstrate its convergence, speed and accuracy through a series of examples. In § 4, finally, we use our algorithm to study orthorhombic and monoclinic polycrystalline systems, with an emphasis on characterization of texture-dependent behaviour.

Other studies of mathematical models of martensitic phase transitions in polycrystals include Bhattacharya & Kohn (1996, 1997), Boyd & Lagoudas (1994), Bruno &

Goldsztein (1999), Bruno *et al*. (1996), Gall & Sehitoglu (1999), Inoue *et al*. (1996), Lu & Weng (1998), Shu & Bhattacharya (1998), Smyshlyeav & Willis (1998), Sun & Hwang (1993*a*, *b*), Thamburaja & Anand (2001) and Zhao *et al*. (1998).

2. The mathematical model

In this section we provide a brief description of our mathematical model of martensitic transformations in polycrystals; additional details can be found in Bruno *et al*. (1996), Smyshlyeav & Willis (1998) and Bruno & Goldsztein (1999).

(*a*) *Martensitic transformations in single crystals*

For convenience we use a reference configuration in which the stress-free strain of the austenite is 0. The transformation strain corresponding to the ith variant of martensite is denoted by $\varepsilon^{\mathrm{T}(i)}$. The number M of martensite variants depends on martensite crystalline symmetry: for any pair of transformation strains $\varepsilon^{\mathrm{T}(i)}$ and $\varepsilon^{\mathrm{T}(j)}$, there exists rotation P in the symmetry group of the austenite crystalline lattice such that $\varepsilon^{\mathrm{T}(i)} = P\varepsilon^{\mathrm{T}(j)}P^{-1}$ (Wayman 1964; Wechsler *et al*. 1953).

As mentioned in the introduction, we assume that both the austenite and martensite phases are linearly elastic with isotropic elastic moduli C:

$$C_{ijk\ell} = \mu\left(\frac{2\nu}{1-2\nu}\delta_{ij}\delta_{k\ell} + \delta_{ik}\delta_{j\ell} + \delta_{i\ell}\delta_{jk}\right). \tag{2.1}$$

In what follows, the region occupied by the single crystal is denoted by Δ, the displacement vector is denoted by u and its associated linear strain by $\varepsilon = \varepsilon(u)$,

$$\varepsilon_{ij} = \varepsilon_{ij}(u) = \varepsilon_{ij}(x) = \frac{1}{2}\left(\frac{\partial u_i}{\partial x_j} + \frac{\partial u_j}{\partial x_i}\right) = \tfrac{1}{2}(u_{i,j} + u_{j,i}). \tag{2.2}$$

Further, we denote by $\varepsilon^{\mathrm{T}}(x)$ the transformation strain at the point x (i.e. $\varepsilon^{\mathrm{T}} = \varepsilon^{\mathrm{T}}(x) = \varepsilon^{\mathrm{T}(m)}$ if the material at x is the mth martensite variant), so that the stress σ is given by

$$\sigma_{ij} = C_{ijk\ell}(\varepsilon_{k\ell} - \varepsilon^{\mathrm{T}}_{k\ell}). \tag{2.3}$$

The displacement vector u satisfies the equilibrium equations

$$\sigma_{ij,j} = 0; \tag{2.4}$$

for the sake of the present discussion we consider the homogeneous boundary conditions

$$u_i(x) = \varepsilon^0_{ij}x_j \quad \text{for } x \in \partial\Delta. \tag{2.5}$$

The model used in this paper assumes that, under given displacements (2.5), the field of transformation strains $\varepsilon^{\mathrm{T}} = \varepsilon^{\mathrm{T}}(x)$ within the single crystal Δ is selected in such a way as to minimize the elastic energy over all possible arrays of transformation strains (see also Khachaturyan 1966). We will denote this minimum by $E = E(\varepsilon^0)$ and the elastic energy corresponding to a given field of transformation strains ε^{T} by $W = W(\varepsilon^0, \varepsilon^{\mathrm{T}})$. Thus, we have

$$E = E(\varepsilon^0) = \inf_{\varepsilon^{\mathrm{T}}}\{W(\varepsilon^0, \varepsilon^{\mathrm{T}}) : \varepsilon^{\mathrm{T}}(x) \in \{\varepsilon^{\mathrm{T}(1)}, \ldots, \varepsilon^{\mathrm{T}(M)}\} \text{ for all } x\}, \tag{2.6}$$

where

$$W = W(\varepsilon^0, \varepsilon^{\mathrm{T}}) = \frac{1}{2|\Delta|} \int_{\Delta} \sigma_{ij}(x)(\varepsilon_{ij}(x) - \varepsilon^{\mathrm{T}}_{ij}(x))\,\mathrm{d}x. \tag{2.7}$$

The quantity E is called the overall, effective, macroscopic or relaxed energy. As is known, the effective energy E depends only on the applied strain ε^0 and not on the domain Δ.

This definition of the overall energy function needs to be qualified: in general, minimizers of equation (2.6) do not exist, and the effective energy is the *infimum* of all energy values. This fact causes difficulties if an attempt is made to solve (2.6) by means of a straightforward numerical method, since such direct formulations lead to arrays of transformation strains which oscillate with infinitesimally small wavelengths.

If the transformation strains satisfy certain conditions, however, the minimum value in equation (2.6) can be obtained explicitly. To explain this let us define a pair of linear strains $\varepsilon^{(1)}$ and $\varepsilon^{(2)}$ to be compatible if there exists a displacement u defined in an open connected set Δ whose linear strain takes the value $\varepsilon^{(1)}$ in a subset $\Delta_1 \subset \Delta$ and the value $\varepsilon^{(2)}$ in the complement set $\Delta_2 = \Delta - \Delta_1$, where the sets Δ_1 and Δ_2 have non-empty interiors. (As is known, $\varepsilon^{(1)}$ and $\varepsilon^{(2)}$ are compatible if and only if $\varepsilon^{(1)} - \varepsilon^{(2)} = D + D^{\mathrm{t}}$, where D is a tensor of rank one.) If the transformation strains are pairwise compatible (i.e. $\varepsilon^{\mathrm{T}(i)}$ and $\varepsilon^{\mathrm{T}(j)}$ are compatible for every pair (i, j)), then it can be shown that $E(\varepsilon^0) = 0$ for every ε^0 in the set

$$\mathcal{S}_0 = \text{convex hull of } \{\varepsilon^{\mathrm{T}(1)}, \ldots, \varepsilon^{\mathrm{T}(M)}\} \tag{2.8}$$

(see Bhattacharya 1993). More generally, if the transformation strains are pairwise compatible, we have

$$E(\varepsilon^0) = \min_{\varepsilon^{\mathrm{T}} \in \mathcal{S}_0} \tfrac{1}{2}(\varepsilon^0_{ij} - \varepsilon^{\mathrm{T}}_{ij}) C_{ijk\ell}(\varepsilon^0_{k\ell} - \varepsilon^{\mathrm{T}}_{k\ell}). \tag{2.9}$$

In this equation ε^{T} is not a transformation strain but rather the *mesoscopic* average value of the transformation strains over a length-scale much smaller than the one associated with the size of the region Δ and at the same time much larger than the microscopic length-scale, that is, the length-scale associated with the oscillations developed by the minimizers. Since here we are not concerned with the detailed behaviour at microscopic length-scales, we will still refer to ε^{T} as the transformation strain even though it really is its local average.

(*b*) *Martensitic transformations in polycrystals*

A polycrystal is a collection of bonded single crystalline grains. Thus, the orientation of the crystallographic axes of the material is constant within each grain but it varies from grain to grain; the orientation field is determined by a rotation-valued function $R = R(x)$. If $\mathcal{S}_0$ is the set of transformation strains of the reference single crystal, the set of transformation strains of a single crystal with orientation R is $R\mathcal{S}_0R^{\mathrm{T}}$. Therefore, the field of transformation strains ε^{T} in a polycrystal must satisfy the pointwise restriction $\varepsilon^{\mathrm{T}}(x) \in R(x)\mathcal{S}_0R^{\mathrm{T}}(x)$, and the effective energy associated with a polycrystal contained in a region Ω is given by

$$E = E(\varepsilon^0) = \min_{\varepsilon^{\mathrm{T}}} \{W(\varepsilon^0, \varepsilon^{\mathrm{T}}) : \varepsilon^{\mathrm{T}}(x) \in R(x)\mathcal{S}_0R^{\mathrm{T}}(x) \text{ for all } x \in \Omega\}. \tag{2.10}$$

As mentioned in the Introduction, in this paper we are concerned with the homogenization limit, in which the size of the grains is much smaller than the size of the polycrystal; the small grain limit is implicit in equation (2.10).

The elastic energy W is a function of the applied strain ε^0 and the transformation strains $\varepsilon^{\mathrm{T}}(x)$. In what follows we will use the relation

$$W = W(\varepsilon^0, \varepsilon^{\mathrm{T}}) = W_1(\varepsilon^0, \varepsilon^{\mathrm{T(av)}}) + W_2(\varepsilon^{\mathrm{T}} - \varepsilon^{\mathrm{T(av)}}), \tag{2.11}$$

where

$$W_1 = \tfrac{1}{2} C_{ijk\ell}(\varepsilon^0_{ij} - \varepsilon^{\mathrm{T(av)}}_{ij})(\varepsilon^0_{k\ell} - \varepsilon^{\mathrm{T(av)}}_{k\ell}), \tag{2.12}$$

$\varepsilon^{\mathrm{T(av)}}$ denotes the average of ε^{T},

$$\varepsilon^{\mathrm{T(av)}} = \frac{1}{|\Omega|}\int_\Omega \varepsilon^{\mathrm{T}}(x)\,\mathrm{d}x, \tag{2.13}$$

and

$$\begin{aligned} W_2 = {} & \frac{1}{2|\Omega|} C_{ijk\ell}\int_\Omega (\varepsilon^{\mathrm{T}}_{ij}(x) - \varepsilon^{\mathrm{T(av)}}_{ij})(\varepsilon^{\mathrm{T}}_{k\ell}(x) - \varepsilon^{\mathrm{T(av)}}_{k\ell})\,\mathrm{d}x \\ & + \frac{C_{ijru}C_{tsk\ell}}{2|\Omega|}\int_\Omega \mathrm{d}x\,(\varepsilon^{\mathrm{T}}_{ij}(x) - \varepsilon^{\mathrm{T(av)}}_{ij})\left\{\int_\Omega \mathrm{d}y\,\Gamma_{rt,s}(x-y)(\varepsilon^{\mathrm{T}}_{k\ell}(y) - \varepsilon^{\mathrm{T(av)}}_{k\ell})\right\}_{,u}. \end{aligned} \tag{2.14}$$

In the last equation Γ denotes the three-dimensional Green function

$$\Gamma_{ij} = \frac{1}{4\pi\mu}\frac{\delta_{ij}}{r} - \frac{r_{,ij}}{16\pi\mu(1-\nu)}, \tag{2.15}$$

where $r = \sqrt{x_1^2 + x_2^2 + x_3^2}$.

These expressions reduce our full optimization problem (2.10) to minimization over the array of transformation strains only—since the minimization needed for solution of the linear elasticity problem is accounted for exactly by means of equations (2.11)–(2.14). Detailed derivations of these equations are given in Bruno *et al.* (1996), Smyshlyeav & Willis (1998) and Bruno & Goldsztein (1999).

3. The numerical method

Our numerical method, in its most general form, has been described in Bruno & Goldsztein (1999); in what follows we restrict our discussion to an idealized polycrystalline geometry composed of cubic grains, with $\varepsilon^{\mathrm{T}}(x)$ constant within each grain. More precisely, our polycrystal occupies the region in space Ω

$$\Omega = [0,1]^3 \tag{3.1}$$

and the grains G are of the form

$$G = G_{ijk} = h(i,j,k) + [0,h]^3 \quad \text{with } 0 \leqslant i,j,k < n \text{ and } h = n^{-1}. \tag{3.2}$$

We remark that our results do not depend on the shape of the polycrystal Ω, and we point out that equations (2.11)–(2.14) are only valid in the limit $n \to \infty$; in our numerical calculations we take n to be a large integer. Under our assumptions, and

denoting by $\varepsilon^{\mathrm{T}}(G)$ the value that ε^{T} takes in the grain G, we have $W_2 = \lim_{h\to 0} W_2^h$, where

$$W_2^h = \sum_{G,H \text{ grains}} w_{ijk\ell}^{GH}(\varepsilon_{ij}^{\mathrm{T}}(G) - \varepsilon_{ij}^{\mathrm{T(av)}})(\varepsilon_{k\ell}^{\mathrm{T}}(H) - \varepsilon_{k\ell}^{\mathrm{T(av)}}) \tag{3.3}$$

with

$$w_{ijk\ell}^{GH} = \frac{1}{2|\Omega|} C_{ijru} C_{tsk\ell} \int_G \left\{ \int_H \Gamma_{rt,s}(x-y)\,\mathrm{d}y \right\}_{,u} \mathrm{d}x + \frac{C_{ijk\ell}}{2|\Omega|}|G|\delta_{GH}, \tag{3.4}$$

and

$$\delta_{GH} = \begin{cases} 1 & \text{if } G = H, \\ 0 & \text{otherwise.} \end{cases} \tag{3.5}$$

The coefficients $w_{ijk\ell}^{GH}$, which can be obtained analytically for cubic grains, are given in Appendix A.

(*a*) *Convergent sequence of approximations*

Given any two grains G_1 and G_2,

$$G_1 = h(i_1, j_1, k_1) + [0,h]^3 \quad \text{and} \quad G_2 = h(i_2, j_2, k_2) + [0,h]^3, \tag{3.6}$$

we define the distance between them as

$$\mathrm{dist}(G_1, G_2) = \max\{|i_1 - i_2|, |j_1 - j_2|, |k_1 - k_2|\}. \tag{3.7}$$

We now introduce the following sequence of approximations of W_2^h:

$$W_2^{h,r} = \sum_{\mathrm{dist}(G,H)<r} w_{ijk\ell}^{GH}(\varepsilon_{ij}^{\mathrm{T}}(G) - \varepsilon_{ij}^{\mathrm{T(av)}})(\varepsilon_{k\ell}^{\mathrm{T}}(H) - \varepsilon_{k\ell}^{\mathrm{T(av)}}). \tag{3.8}$$

We clearly have $W_2^h = \lim_{r\to\infty} W_2^{h,r}$. As demonstrated in Bruno & Goldsztein (1999) for two-dimensional polycrystals, small values of r provide excellent approximations $W_2^{h,r}$ of W_2^h; our calculations below show that this is also the case in the three-dimensional case considered presently. This fact allows us to replace W_2^h by $W_2^{h,r}$ (with r small) and, as a result, to reduce the complexity of our numerical method to $O(N)$ operations, where $N = n^3$ is the number of grains that make up the polycrystal. This sequence of approximations can be regarded as a generalized mean field approximation, in the sense that replacing W_2^h by $W_2^{h,r}$ is equivalent to approximating the displacement in any grain G by the displacement produced under the same boundary conditions, with the same $\varepsilon^{\mathrm{T}}(H)$ for all grains H such that $\mathrm{dist}(G,H) < r$, and replacing $\varepsilon^{\mathrm{T}}(H)$ by $\varepsilon^{\mathrm{T(av)}}$ for all other grains. We emphasize, however, that as r is increased the $W_2^{h,r}$ provide a *convergent* sequence of approximations—in contrast to the essentially limited accuracy implicit in the self-consistent approximations. A rationale for the remarkable accuracy of the approximations $W_2^{h,r}$ is given in Bruno & Goldsztein (1999).

(*b*) *Minimization algorithm*

In what follows, we denote by $R(G)$ the orientation of the grain G. With this notation we translate the convergent approximations of the previous section into corresponding approximations $E^{h,r}(\varepsilon^0)$ of $E(\varepsilon^0)$

$$E^{h,r}(\varepsilon^0) = \min\{W_1 + W_2^{h,r} : \varepsilon^{\mathrm{T}}(G) \in R(G)\mathcal{S}_0 R^{\mathrm{T}}(G) \text{ for all grains } G\} \tag{3.9}$$

(see equations (2.12), (3.8) and (2.8)).

Our minimization algorithm proceeds as follows: given a grain G, the energy $W^{h,r} = W_1 + W_2^{h,r}$ is minimized with respect to $\varepsilon^{\mathrm{T}}(G) \in R(G)\mathcal{S}_0 R^{\mathrm{T}}(G)$ (see equation (3.9)), while $\varepsilon^{\mathrm{T}}(H)$ is held fixed for all other grains ($H \neq G$). This defines a new value of $\varepsilon^{\mathrm{T}}(G)$ which is used in all subsequent calculations. Using a visiting schedule, the transformation strains ε^{T} in all the grains of the polycrystal are updated once per iteration. (Our computations use a lexicographic visiting schedule, but other possibilities may be as efficient.) This process is repeated until the minimum is obtained with the required accuracy.

As shown by the examples below, our simple minimization algorithm is very efficient: it converges in a small number of iterations. As discussed in Bruno & Goldsztein (1999), this good quality is linked to a certain lack of correlation in the minimizing arrays of transformation strains.

(*c*) *Complexity*

Let us consider a given array ε^{T} of transformation strains and the corresponding value $W^{h,r} = W_1 + W_2^{h,r}$ of the elastic energy under given applied strains ε^0, and let G be a given grain. If we change the value of $\varepsilon^{\mathrm{T}}(G)$ to $\varepsilon^{\mathrm{T}}_{\mathrm{new}}(G)$,

$$\varepsilon^{\mathrm{T}}_{\mathrm{new}}(G) = \Delta\varepsilon^{\mathrm{T}} + \varepsilon^{\mathrm{T}}(G), \tag{3.10}$$

the value of the energy $W^{h,r}$ changes to a new value W_{new},

$$W^{h,r}_{\mathrm{new}} = \Delta W + W^{h,r}. \tag{3.11}$$

This change in energy ΔW is a quadratic function of $\Delta\varepsilon^{\mathrm{T}}$

$$\Delta W = A_{ijk\ell}\Delta\varepsilon^{\mathrm{T}}_{ij}\Delta\varepsilon^{\mathrm{T}}_{k\ell} + 2B_{ij}\Delta\varepsilon^{\mathrm{T}}_{ij}. \tag{3.12}$$

In Appendix B we present explicit expressions for the coefficients $A_{ijk\ell}$ and B_{ij}, and, in particular, we show that these coefficients can be computed in $O(r^3)$ operations. Clearly, the minimization with respect to $\varepsilon^{\mathrm{T}}(G)$ (or, equivalently, with respect to $\Delta\varepsilon^{\mathrm{T}}(G)$) under the constraint (3.9) requires $O(1)$ operations once we have the coefficients $A_{ijk\ell}$ and B_{ij}. Thus, an iteration is completed in $O(Nr^3)$ operations. As shown below, a small number of iterations and small value of r suffice to obtain small relative errors, and thus the complexity of our method is $O(N)$ with a small constant.

(*d*) *Local minimization*

Introducing the notation $x_1 = \Delta\varepsilon_{11}$, $x_2 = \Delta\varepsilon_{12}$, $x_3 = \Delta\varepsilon_{13}$, $x_4 = \Delta\varepsilon_{22}$ and $x_5 = \Delta\varepsilon_{23}$, the minimization problem whose minimum is the optimal value of ΔW (see (3.11)) can be expressed in the form

$$\min_{\boldsymbol{x}\in\mathbb{R}^5}\{\Delta W = a_{ij}x_i x_j + 2b_i x_i : p_{kj}x_j \geqslant q_k, 1 \leqslant i, j \leqslant 5 \text{ and } 1 \leqslant k \leqslant N_{\mathrm{c}}\}. \tag{3.13}$$

Note that the coefficients a_{ij} and b_i depend on the coefficients $A_{ijk\ell}$ and B_{ij} of equation (3.12) and the orientation of the grain G, whereas the linear-constraint coefficients p_{kj} and q_k depend on the set of transformation strains $\{\varepsilon^{\mathrm{T}(1)}, \ldots, \varepsilon^{\mathrm{T}(M)}\}$. In particular, when the austenite has cubic symmetry and the martensite has orthorhombic symmetry the number of constraints is $N_{\mathrm{c}} = 6$, while for monoclinic martensite we have $N_{\mathrm{c}} = 25$.

Since there are only five minimization variables in (3.13), and since the number of constraints N_{c} is also relatively low (6 or 25 in the examples we consider), we use the direct (i.e. non-iterative) method of Theil & Van de Panne (1960) to solve the minimization problem (3.13).

(*e*) *Convergence*

We now demonstrate the convergence of our method through an application to the following example: assuming orthorhombic martensite, we take the reference misfit to be given by

$$\varepsilon^{\mathrm{T}(1)} = \begin{bmatrix} \alpha & \delta & 0 \\ \delta & \alpha & 0 \\ 0 & 0 & \beta \end{bmatrix}, \tag{3.14}$$

with $\alpha = 0.04$, $\beta = -0.08$ and $\delta = 0.02$. These values of the material parameters are similar to those found in some Cu–Al alloys (Otsuka & Shimizu 1974). The complete set of (six) transformation strains for this material are then $\{R\varepsilon^{\mathrm{T}(1)}R^{-1} : R \in$ group of symmetry of the cubic lattice$\}$. As is known, these transformation strains are pairwise compatible and thus we can directly apply our methods to this case. Further, we assume random crystallographic orientations with a uniform probability distribution. More precisely, if we parametrize the rotation matrix R through Euler angles θ, ρ and γ, $R = R(\theta, \rho, \gamma)$,

$$R = \begin{bmatrix} \cos\theta\cos\rho & -\sin\theta\cos\gamma - \cos\theta\sin\rho\sin\gamma & \sin\theta\sin\gamma - \cos\theta\sin\rho\cos\gamma \\ \sin\theta\cos\rho & \cos\theta\cos\gamma - \sin\theta\sin\rho\sin\gamma & -\cos\theta\sin\gamma - \sin\theta\sin\rho\cos\gamma \\ \sin\rho & \cos\rho\sin\gamma & \cos\rho\cos\gamma \end{bmatrix},$$

where $-\pi < \theta \leqslant \pi$, $-\pi < \gamma \leqslant \pi$ and $-\pi/2 \leqslant \rho \leqslant \pi/2$, the uniform probability distribution is given by

$$p = p(\theta, \rho, \gamma) = \frac{\cos\rho}{8\pi^2}. \tag{3.15}$$

Finally, we take $\nu = 0.25$, $\mu = 100$ GPa and

$$\varepsilon^0 = \begin{bmatrix} 0.02 & 0 & 0 \\ 0 & -0.01 & 0 \\ 0 & 0 & -0.01 \end{bmatrix}. \tag{3.16}$$

In table 1 we show the value of the energy $W^{h,r}$ after I iterations ($I = 0, 1, 2, \ldots$) for different values of n and r. This table illustrates some useful properties of our convergent approximations: the number of iterations required to achieve any desired accuracy is independent of n and increases with r but it remains bounded (by a small number).

The convergence of the energy $E^{h,r}$ as both n and r tend to ∞, in turn, is illustrated in table 2, where we display $E^{h,r}$ for different values of n and r.

Table 1. *Energy values* $W^{h=1/n,r}$ *(in* MPa*) as a function of the number* I *of iterations*

	$N = 20^3$		$N = 80^3$	
I	$r = 1$	$r = 8$	$r = 1$	$r = 8$
0	60	60	60	60
1	5.17	5.10	5.15	5.08
2	2.34	2.08	2.32	2.02
3	2.30	1.94	2.28	1.89
4	2.30	1.93	2.28	1.88
5	2.30	1.92	2.28	1.87
6	2.30	1.92	2.28	1.87

Table 2. *Energies* $E^{h=1/n,r}$ *(in* MPa*) for different values of* n *and* r

r	$N = 10^3$	$N = 20^3$	$N = 40^3$	$N = 80^3$
1	2.19	2.30	2.28	2.28
2	1.96	2.06	2.02	2.02
4	1.87	1.96	1.91	1.90
8		1.92	1.88	1.87

Table 3. *Computing times to obtain* $E^{h,r}$ *with three digits of accuracy, in seconds*

r	$N = 10^3$	$N = 20^3$	$N = 40^3$	$N = 80^3$
1	1.25	10	80	642
2	3.07	25.7	210	1 702
4	18.84	187	1 720	14 230
8		1500	15 560	126 142

In table 3, finally, we show the computing times (using a 300 MHz PC) necessary to obtain the overall energy with a relative error smaller than 10^{-3} for different values of n and r. In particular, this table illustrates the $O(N)$ complexity of our method.

These examples support our claims that the numerical method requires a small number of iterations, a small value of r (associated with our sequence to approximations) and that the complexity of the method is linear in the number grains. We note that there is an unavoidable fluctuation in the values of $E^{h,r}$, which results from the statistical fluctuations present in our finite samples.

4. Applications

In this section we apply our method to study the dependence of the polycrystalline phase transitions on texture for two of the most important misfit symmetry classes: orthorhombic and monoclinic. The misfits to be considered are described in the following sections. For generality we will use a variety of textures, as discussed in what follows.

The texture of a polycrystal is characterized by a probability distribution for the array of crystalline orientations in a polycrystal; we will assume the crystallographic orientations in our examples are given by independent identically distributed random variables with probability distribution p. We will consider families of probability distributions parametrized by a parameter $\eta \in [0,1]$, $p = p_\eta$, each one defining a polycrystal, in such a way that $\eta = 1$ corresponds to the uniform probability (see equations (3.15)) and $\eta = 0$ corresponds to a delta function (i.e. all the grains have the same orientation and thus the polycrystal behaves as a single crystal). Parametrizing the rotation matrix R as in § 3, the probability distribution p_η we use is given by

$$p_\eta = p_\eta(\theta, \rho, \gamma) = \begin{cases} \dfrac{\cos\rho}{8\pi^2\eta^3} & \text{if } |\theta| \leqslant \eta\pi,\ |\gamma| \leqslant \eta\pi \text{ and } |\sin\rho| \leqslant \eta, \\ 0 & \text{otherwise;} \end{cases} \tag{4.1}$$

clearly, the parameter η is a measure of the variation in the crystallographic orientations from grain to grain.

(*a*) *Cubic-to-orthorhombic transformation*

In this section we consider a polycrystal with basic transformation strains given by equation (3.14) (with parameters values as given in the text following that equation), and with elastic constants $\nu = 0.25$ and $\mu = 100$ GPa.

(i) *Applied strains*

We will study the response of the polycrystals under the following two families of applied strains:

$$\varepsilon_1^0 = \varepsilon_1^0(x) = x\varepsilon^{\mathrm{T}(1)}, \tag{4.2}$$

where $\varepsilon^{\mathrm{T}(1)}$ is the transformation strain given in equation (3.14) and

$$\varepsilon_2^0 = \varepsilon_2^0(x) = xA, \tag{4.3}$$

with

$$A = \begin{bmatrix} -0.000\,71 & 0.006\,43 & 0 \\ 0.006\,43 & -0.000\,71 & 0 \\ 0 & 0 & 0.001\,42 \end{bmatrix}. \tag{4.4}$$

Our motivation in the choice of these two families of applied strains is as follows: the energy in a single crystal oriented in accordance with the rotation matrix R under the family of applied strains (4.2) takes its minimum value for $R = I$. Thus, for a polycrystal with texture given by (4.1) the applied strains (4.2) should be accommodated more easily (with lower energy) as η decreases—since decreasing values of η tend to orient all grains in directions closer to the optimal $R = I$. The opposite effect is to be expected when the family of applied strains (4.3) is used: in strain

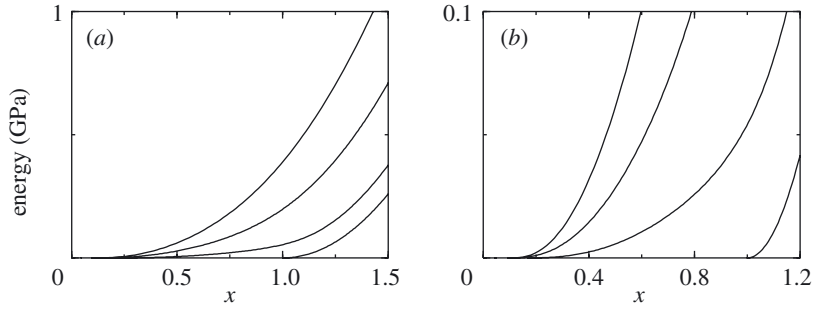

Figure 1. Energy curves $E(\varepsilon_1^0(x))$ versus x corresponding to the textures $\eta = 0$, $\eta = 0.1$, $\eta = 0.2$ and $\eta = 1$ for (a) $0 \leqslant x \leqslant 1.5$ and (b) $0 \leqslant x \leqslant 1.2$. In all cases larger values of η correspond to higher-energy values.

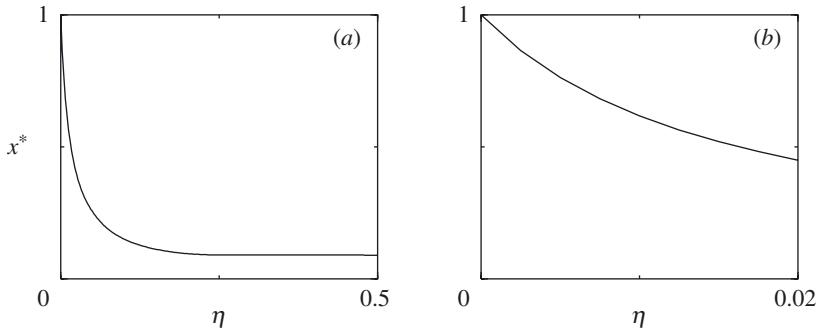

Figure 2. Plot of x^* versus η for (a) $0 \leqslant \eta \leqslant 0.5$ and (b) $0 \leqslant \eta \leqslant 0.02$. For a texture η the energy $E(\varepsilon_1^0(x))$ vanishes for $0 \leqslant x \leqslant x^*(\eta)$.

space, the tensor A points in a direction of maximal increase for the elastic energy of a single crystal oriented according to $R = I$.

(ii) *Energy–strain and stress–strain curves*

In figure 1 we show the energy curves $E = E(\varepsilon_1^0(x))$ versus x for textures corresponding to $\eta = 0$, $\eta = 0.1$, $\eta = 0.2$ and $\eta = 1$. As expected from our previous discussion, the energy values increase with η.

To interpret these curves it is useful to consider the fact that, in the present case, the set of transformation strains generates the five-dimensional space of deviatoric strains. Thus, for any texture, the set of applied strains for which the energy is zero has a non-empty interior in the space of deviatoric strains. In particular, for each η, there exists $x^* = x^*(\eta) > 0$ such that $E(\varepsilon_1^0(x)) = 0$ for all $0 \leqslant x \leqslant x^*$ when the texture is determined by η. Figure 2 shows a plot of x^* versus η.

The energy cannot be measured directly in experiments, and it is therefore of interest to evaluate the macroscopic or average stress as a function of the applied strain. Since our numerical method provides the microscopic behaviour of the polycrystal, obtaining the average stress is simple. Figure 3 shows a plot of the average of the $(1, 1)$ component of the stress as a function of x. The applied strain is given by (4.2) and the texture corresponds to $\eta = 0$, $\eta = 0.1$, $\eta = 0.2$ and $\eta = 1$.

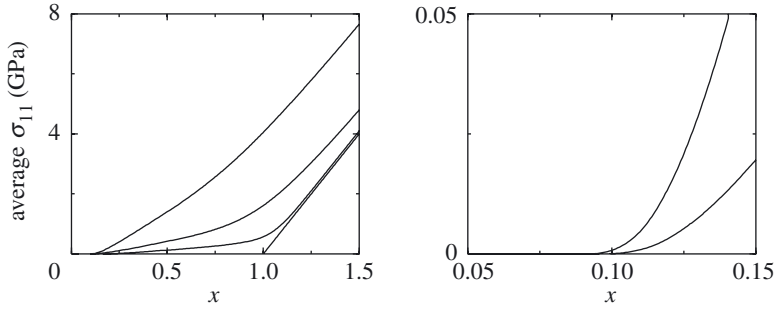

Figure 3. Stress–strain curves: average of σ_{11} versus x (when the applied strains $\varepsilon_1^0(x)$ are given by (4.2)) corresponding to the textures (from lowest to highest curve) $\eta = 0$, $\eta = 0.1$, $\eta = 0.2$ and $\eta = 1$. The right-hand figure corresponds to the textures $\eta = 0.2$ and $\eta = 1$.

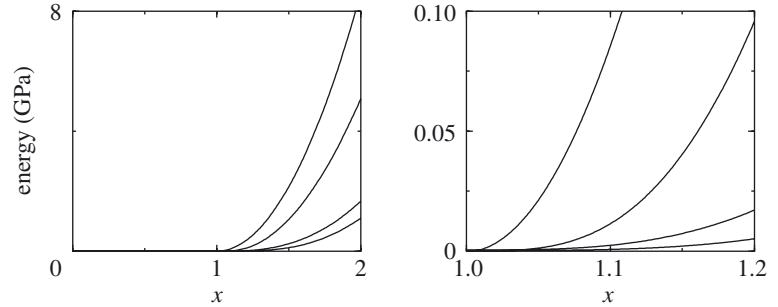

Figure 4. Energy curves $E(\varepsilon_2^0(x))$ versus x corresponding to the textures (from lowest to highest curve) $\eta = 1$, $\eta = 0.2$, $\eta = 0.1$ and $\eta = 0$.

Figure 4 shows $E(\varepsilon_2^0(x))$ versus x for different values of η. In accordance to our previous discussion, the energy decreases as η increases.

(iii) *Recoverable strains*

The strain tensor $\varepsilon^{\mathrm{T}(1)}$ of equation (3.14) gives rise to a maximum linear deformation of 8%; in the following discussion it will be relevant to consider the elastic energy E_* arising in an elastic material, with the constants ν and μ presently under consideration, as a result of an *elastic* strain (i.e. *without phase transition*) equal to an eighth of $\varepsilon^{\mathrm{T}(1)}$, or, roughly speaking, a 1% deformation. This quantity is given by

$$E_* = \tfrac{1}{2}\varepsilon^{\mathrm{T}(1)} C \varepsilon^{\mathrm{T}(1)}/8^2 = \varepsilon^{\mathrm{T}(1)} C \varepsilon^{\mathrm{T}(1)}/128 = 0.0163\ \mathrm{GPa}.$$

This energy value is relevant for our discussion of recoverable strains. Indeed, as is known, each one of the phases of the CuAl shape-memory alloys can withstand fully recoverable elastic strains (without phase transition) of the order of 1% (see, for example, Otsuka & Shimizu 1986). We thus assume that the applied strains that can be recovered, with or without phase transitions, are those whose energy is less than 0.0163 GPa. According to this criterion the applied strains of the form (4.2) are recoverable provided $0 \leqslant x \leqslant x_{\mathrm{orth}}(\eta)$, where $E(\varepsilon_1^0(x_{\mathrm{orth}})) = 0.0163$ GPa. In particular, our prediction is that the maximum recoverable strains for the various textures considered above are given by $x_{\mathrm{orth}}(0) = 1.1$, $x_{\mathrm{orth}}(0.1) = 0.69$, $x_{\mathrm{orth}}(0.2) = 0.42$ and $x_{\mathrm{orth}}(1) = 0.32$.

(*b*) *Cubic to monoclinic transformation*

We now turn our attention to a material undergoing cubic to monoclinic transformations. In detail, we assume that the reference transformation strain is given by

$$\varepsilon^{\mathrm{T}(1)} = \begin{bmatrix} 0.025 & 0.06 & 0.04 \\ 0.06 & 0.025 & 0.04 \\ 0.04 & 0.04 & -0.05 \end{bmatrix}. \tag{4.5}$$

These material parameters are similar to those associated with some NiTi alloys (Knowles & Smith 1981); as for the elastic constants we again use the arbitrary but reasonable values $\nu = 0.25$ and $u = 100$ GPa.

A monoclinic material has 12 different transformation strains, and, unlike the orthorhombic case treated in the previous section, here the transformation strains are not pairwise compatible. An evaluation of polycrystalline effective energies requires knowledge about the effective energies for single crystals; unfortunately, because of the lack of pairwise compatibility, the effective energy of monoclinic single crystals is not known. Interestingly, however, tight upper bounds on the effective energy of monoclinic single crystals have been provided recently by Goldsztein (2001), which, as shown in what follows, allow us to develop tight upper and lower bounds for the polycrystalline energy. To do this we first approximate the effective energy of the single crystal by its convexification E_{c} and we compute the polycrystalline energy E^{l} which results as E_{c} is used instead of the basic single crystal energy function. Clearly, E^{l} is a lower bound for the true polycrystalline energy. We then use the results of Goldsztein (2001) to bound the errors produced by this approximation and to produce an upper bound E^{u} for the polycrystalline energy.

In detail, Goldsztein (2001) showed that, for any applied strain, the difference between the effective energy and its convexification is bounded by

$$\tfrac{1}{4}(1+\nu)\mu \max_{1 \leqslant i < j \leqslant M} \{\min\{z^2 : z \text{ eigenvalue of } \varepsilon^{\mathrm{T}(i)} - \varepsilon^{\mathrm{T}(j)}\}\}. \tag{4.6}$$

For the material parameters under consideration, this quantity equals 0.0102 GPa. Thus, in the present context, to obtain upper bounds E^{u} on the energy E it suffices to add 0.0102 GPa to the lower bound E^{l}. The bounds E^{l} and E^{u} are displayed in figure 5 as solid and dashed curves, respectively.

We consider the family of applied strains

$$\varepsilon_3^0 = \varepsilon_3^0(x) = x\varepsilon^{\mathrm{T}(1)} \tag{4.7}$$

with $\varepsilon^{\mathrm{T}(1)}$ as in (4.5) and we use, again, textures given by the probability distributions (4.1). The solid curves in figure 5 show the lower bound $E^{\mathrm{l}}(\varepsilon_3^0(x))$ versus x for values of $\eta = 1$, $\eta = 0.2$, $\eta = 0.1$ and $\eta = 0$.

The qualitative character of these curves is similar to that obtained for the polycrystal undergoing cubic-to-orthorhombic transformations (compare figure 5 with figure 1). We note that the lower bound E^{l} remains equal to zero for larger fractions x of the basic transformation strain than the energy E does for the polycrystal undergoing cubic-to-orthorhombic transformation. This is clearly seen in figure 6, where we have plotted x^* versus η (as before, $x^*(\eta)$ is the largest value of x for which $E(\varepsilon_3^0(x)) = 0$).

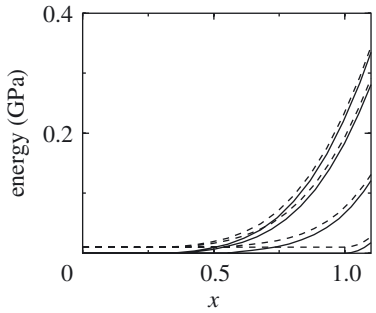

Figure 5. Solid curves, lower bounds $E^{\mathrm{l}}(\varepsilon_3^0(x))$; dashed curves, upper bounds $E^{\mathrm{u}}(\varepsilon_3^0(x))$. The four pairs of curves correspond, from lowest to highest, to the textures $\eta = 0$, $\eta = 0.1$, $\eta = 0.2$ and $\eta = 1$.

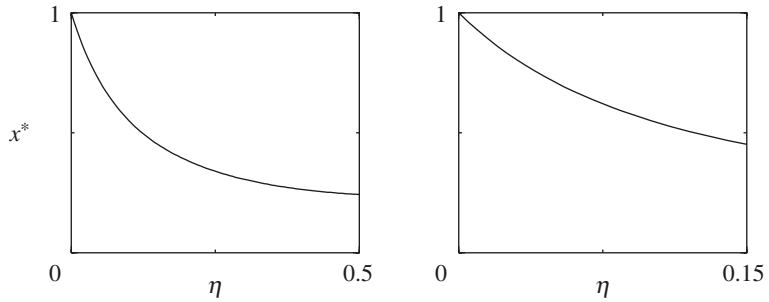

Figure 6. Plot of x^* versus η. The energy $E(\varepsilon_3^0(x))$ is equal to 0 for $0 \leqslant x \leqslant x^*$ when the texture is given by η.

From figures 2 and 6 we see that the value x^* is less than 0.5 for values of η greater than 0.02 for the polycrystal undergoing cubic-to-orthorhombic transformation, while x^* remains greater than 0.5 for values of η smaller than 0.14 in the case in which the polycrystal undergoes cubic to monoclinic transformations. This difference can be easily understood as follows. Consider the norm in the space of strains $\|\varepsilon\|^2 = \varepsilon C\varepsilon$. All the transformation strains $\varepsilon^{\mathrm{T}(i)}$ have the same norm. The number of transformation strains is 6 for materials undergoing cubic-to-orthorhombic transformation and 12 for materials undergoing cubic to monoclinic transformations. Thus, we expect the convex hull of the transformation strains $\mathcal{S}_0$ of material with monoclinic symmetry to be closer to a sphere than the convex hull of the transformation strains of material with the orthorhombic symmetry. In other words, the phase transition in the orthorhombic single crystal is more anisotropic than that in the monoclinic single crystal.

(i) *Recoverable strains*

The strain tensor $\varepsilon^{\mathrm{T}(1)}$ of equation (4.5) gives rise to a maximum linear deformation of 10%; in the following discussion, we consider the elastic energy E_* arising in an elastic material, with the constants ν and μ presently under consideration, as a result of an *elastic* strain (i.e. *without phase transition*) equal to a tenth of $\varepsilon^{\mathrm{T}(1)}$, that is, roughly speaking, a 1% deformation. This quantity is given by

$$E_* = \tfrac{1}{2}\varepsilon^{\mathrm{T}(1)} C \varepsilon^{\mathrm{T}(1)}/10^2 = \varepsilon^{\mathrm{T}(1)} C \varepsilon^{\mathrm{T}(1)}/200 = 0.0174 \text{ GPa}.$$

As in the case of the orthorhombic transformation, we consider the 1% *elastic* strain energy value, since each one of the phases of a TiNi shape-memory alloys can recover from elastic strains of the order of 1% (see, for example, Otsuka & Shimizu 1986; Leo *et al*. 1993). In what follows we thus assume that, in the polycrystal under consideration, the applied strains from which the material can recover are those which give rise to an energy value of less than 0.0174 GPa.

Clearly, the dashed curves can be used to obtain *lower* bounds on the recoverable strains predicted by our criterion. Based on our recoverability assumption we obtain that the applied strains of the form (4.7) are recoverable for at least $0 \leqslant x \leqslant x_{\mathrm{mon}}(\eta)$, where $x_{\mathrm{mon}}(0) = 1.059$, $x_{\mathrm{mon}}(0.1) = 0.686$, $x_{\mathrm{mon}}(0.2) = 0.505$ and $x_{\mathrm{mon}}(1) = 0.468$.

5. Final remarks

In this paper we introduced a numerical method for the simulation of martensitic transformations in polycrystals. We have showed that this method can be used effectively to produce constitutive relations for textured polycrystals. Further refinements of the numerical approach are desirable and possible. These include consideration of anisotropic elastic moduli and spatial variations of the local average of transformation strains within each grain.

Further, we considered a criterion for recoverability of strains in martensitic polycrystals, which considers a strain recoverable if the associated overall energy does not exceed the energy values arising in a polycrystal with the same elastic constants but incapable of undergoing phase transitions. Using, this criterion, our numerical method provides a tool to predict the set of recoverable strains.

This work was sponsored by the Air Force Office of Scientific Research, Air Force Materials Command, USAF, under grant numbers F49620-96-1-0008 and F49620-99-1-0010. The authors gratefully acknowledge support from NSF (through an NYI award). O.P.B. gratefully acknowledges support from NSF (through contract numbers DMS-9523292 and DMS-9816802) and from the Powell Research Foundation. The US Government is authorized to reproduce and distribute reprints for governmental purposes notwithstanding any copyright notation thereon. The views and conclusions contained herein are those of the authors and should not be interpreted as necessarily representing the official policies or endorsements, either expressed or implied, of the Air Force Office of Scientific Research or the US Government.

Appendix A. Interaction coefficients

In this appendix we present explicit algebraic expressions for the coefficients $w_{ijk\ell}^{GH}$ of equation (3.4). Let the grains G and H be of the form

$$G = h(g_1, g_2, g_3) + [0, h]^3 \quad \text{and} \quad H = h(h_1, h_2, h_3) + [0, h]^3.$$

We define $\boldsymbol{k} = (k_1, k_2, k_3) = (g_1 - h_1, g_2 - h_2, g_3 - h_3)$. If we fix h, it is clear that the coefficients $w_{ijk\ell}^{GH}$ depend only on $\boldsymbol{k}$. Defining

$$J_{rtsu}(\boldsymbol{k}) = \int_G \left\{ \int_H \Gamma_{rt,s}(x - x')\,\mathrm{d}x' \right\}_{,u} \mathrm{d}x,$$

algebraic manipulation shows that

$$J_{rtsu}(\boldsymbol{k}) = \frac{1}{16\pi\mu(1-\nu)} \square b_{rtsu}(\boldsymbol{k}) - \frac{\delta_{rt}}{\pi\mu} \square a_{su}(\boldsymbol{k}),$$

where the symbol $\square$ denotes the operation

$$\square f(\boldsymbol{k}) = \sum_{\substack{0\leqslant i_j\leqslant 1,\\ 1\leqslant j\leqslant 6}} (-1)^{\sum_{1\leqslant j\leqslant 6} i_j} f((k_1+i_1-i_2, k_2+i_3-i_4, k_3+i_5-i_6)h),$$

and the functions a_{ij} and $b_{ijk\ell}$ are given by

$$\begin{aligned}
a_{33} &= -xyz\tan^{-1}\left(\frac{xy}{rz}\right) + \tfrac{1}{2}x(y^2-z^2)\log(r+x)\\
&\quad + \tfrac{1}{2}y(x^2-z^2)\log(r+y) + \tfrac{1}{2}z^2 r - \tfrac{1}{6}r^3,\\
a_{32} &= -\tfrac{1}{2}xz^2\tan^{-1}\left(\frac{xy}{rz}\right) - \tfrac{1}{2}xy^2\tan^{-1}\left(\frac{xz}{ry}\right) - \tfrac{1}{6}x^3\tan^{-1}\left(\frac{yz}{rx}\right)\\
&\quad + \tfrac{1}{6}y(3x^2-y^2)\log(r+z) + \tfrac{1}{6}z(3x^2-z^2)\log(y+r)\\
&\quad + xyz\log(x+r) - \tfrac{1}{3}ryz,\\
b_{3333} &= -2xyz\tan^{-1}\left(\frac{xy}{rz}\right) + \tfrac{1}{2}x(y^2-3z^2)\log(r+x)\\
&\quad + \tfrac{1}{2}y(x^2-3z^2)\log(r+y) + \tfrac{3}{2}z^2 r - \tfrac{1}{6}r^3,\\
b_{3332} &= -xz^2\tan^{-1}\left(\frac{xy}{rz}\right) + \tfrac{1}{2}z(x^2-z^2)\log(y+r) + xyz\log(x+r) - \tfrac{1}{2}rzy,\\
b_{3322} &= \tfrac{1}{2}x(y^2+z^2)\log(x+r) + \tfrac{1}{2}x^2 r - \tfrac{1}{3}r^3,\\
b_{3321} &= \tfrac{1}{6}y(y^2+3z^2)\log(x+r) + \tfrac{1}{6}x(x^2+3z^2)\log(y+r)\\
&\quad - \tfrac{1}{3}z^3\tan^{-1}\left(\frac{xy}{rz}\right) + \tfrac{1}{3}ryx,
\end{aligned}$$

where $x = x_1$, $y = x_2$ and $z = x_3$. The rest of the functions a_{ij} and $b_{ijk\ell}$ can be obtained from symmetries of these functions,

$$a_{ji} = a_{ij}, \qquad b_{jik\ell} = b_{ijk\ell}, \qquad b_{k\ell ij} = b_{ijk\ell}, \qquad b_{ikj\ell} = b_{ijk\ell},$$

and by permutations of indices (as in $a_{22}(x,y,z) = a_{33}(x,z,y)$). From $J_{rtsu}(\boldsymbol{k})$, the values of the coefficients in equation (3.4) follow immediately.

Appendix B. Coefficients for the local minimization

In this appendix we present the formula for the coefficients $A_{ijk\ell}$ and B_{ij} of equation (3.12) and we show that they can be computed in $O(r^3)$ operations.

First we note that for any two grains H and J

$$H = h(h_1,h_2,h_3) + [0,h]^3 \quad \text{and} \quad J = h(j_1,j_2,j_3) + [0,h]^3, \tag{B 1}$$

the coefficients $w^{HJ}_{ijk\ell}$ (see equation (3.6)) depend only on

$$\boldsymbol{x} = (x_1,x_2,x_3) = (h_1-j_1, h_2-j_2, h_3-j_3)$$

and thus we use the notation $w_{ijk\ell}(\boldsymbol{x}) = w^{HJ}_{ijk\ell}$. For any grain H of the form (B 1) we define

$$\boldsymbol{p}(H) = (p_1,p_2,p_3), \quad \text{where } p_i = \min\{h_i, N-h_i+1, r\}.$$

We now introduce the following tensors:

$$D_{ijk\ell}(\boldsymbol{y}) = \sum_{1\leqslant m\leqslant 3} \sum_{-y_m<x_m<r} w_{ijk\ell}(\boldsymbol{x}),$$

$$E_{ijk\ell} = \sum_{1\leqslant y_m\leqslant r} \Bigl(\prod_{m=1}^{3} a(y_m)\Bigr) D_{ijk\ell}(\boldsymbol{y}),$$

where

$$a(y) = \begin{cases} 2 & \text{if } y < r, \\ N - 2(r-1) & \text{if } y = r, \end{cases}$$

and

$$\delta^{\mathrm{T}}(\boldsymbol{x}) = h^3 \sum_{H:\boldsymbol{p}(H)=\boldsymbol{x}} \varepsilon^{\mathrm{T}}(H). \tag{B 2}$$

With some algebraic manipulations one can show that

$$A_{ijk\ell} = \tfrac{1}{2}h^6 C_{ijk\ell} + w_{ijk\ell}(\mathbf{0}) - 2h^3 D_{ijk\ell}(\boldsymbol{p}(G)) + h^6 E_{ijk\ell}$$

and

$$b_{ij} = \sum_{\mathrm{dist}(G,H)<r} W^{G,H}_{ijk\ell}(\varepsilon^{\mathrm{T}}_{k\ell}(H) - \varepsilon^{\mathrm{T(av)}}_{k\ell}) - \sum_{1\leqslant x_1,x_2,x_3\leqslant r} D_{ijk\ell}(\boldsymbol{x})\delta_{l\ell}(\boldsymbol{x}) + h^3 E_{ijk\ell}\varepsilon^{\mathrm{T(av)}}_{k\ell} - \tfrac{1}{2}h^3 C_{ijk\ell}(\varepsilon^0_{k\ell} - \varepsilon^{\mathrm{T(av)}}_{k\ell}).$$

In the above formulae we have used the fact that $w_{ijk\ell}(-\boldsymbol{x}) = w_{ijk\ell}(\boldsymbol{x})$. Clearly, these formulae imply that the coefficient $A_{ijk\ell}$ and B_{ij} can be computed in $O(r^3)$ operations. Once $\Delta\varepsilon^{\mathrm{T}}(G)$ is obtained after minimization of equation (3.14) (under the constraints given in (3.11)), the tensors $\varepsilon^{\mathrm{T}}(G)$, $\varepsilon^{\mathrm{T(av)}}$ and $\delta^{\mathrm{T}}(\boldsymbol{p}(G))$ (see equation (B 2)) can be updated in $O(1)$ operations.

References

Bhattacharya, K. 1993 Comparison of the geometrically nonlinear and linear theories of martensitic transformation. *Continuum Mech. Thermodyn.* **5**, 205–242.

Bhattacharya, K. & Kohn, R. V. 1996 Symmetry, texture and the recoverable strain of shape-memory polycrystals. *Acta Mater.* **44**, 529–542.

Bhattacharya, K. & Kohn, R. V. 1997 Elastic energy minimization and the recoverable strain of polycrystalline shape-memory materials. *Arch. Ration. Mech. Analysis* **139**, 99–180.

Boyd, J. & Lagoudas, D. 1994 A thermodynamical constitutive model for the shape memory effect due to transformation and reorientation. In *Proc. SPIE*, vol. 2189, pp. 276–288. The International Society for Optical Engineering.

Bruno, O. P. & Goldsztein, G. H. 1999 A fast algorithm for the simulation of polycrystalline misfits: martensitic transformations in two space dimensions. *Proc. R. Soc. Lond.* A **455**, 4245–4276.

Bruno, O. P. & Goldsztein, G. H. 2000 Numerical simulation of martensitic transformations in two and three-dimensional polycrystals. *J. Mech. Phys. Solids* **8**, 1175–1201.

Bruno, O. P., Reitich, F. & Leo, P. 1996 The overall elastic energy of polycrystalline martensitic solids. *J. Mech. Phys. Solids* **44**, 1051–1101.

Gall, K. & Sehitoglu, H. 1999 The role of texture in tension–compression asymmetry in polycrystalline Ni–Ti. *Int. J. Plasticity* **15**, 69–92.

Goldsztein, G. H. 2001 The effective energy and laminated microstructures in martensitic phase transformations. *J. Mech. Phys. Solids* **49**, 899–925.

Inoue, H., Miwa, N. & Inakazu, W. 1996 Texture and shape memory strains in TiNi alloy sheets. *Acta Mater.* **44**, 4825–4834.

Khachaturyan, A. G. 1966 Some questions concerning the theory of phase transformations in solids. *Sov. Phys. Solid State* **8**, 2163–2168.

Knowles, K. N. & Smith, D. A. 1981 The crystallography of the martensitic transformation in equiatomic nickel–titanium. *Acta Metall.* **29**, 101–110.

Leo, P. H., Shield, T. W. & Bruno, O. P. 1993 Transient heat transfer effects on the pseudoelastic behavior of shape-memory wires. *Acta Metall. Mater.* **41**, 2477–2485.

Lu, Z. & Weng, G. 1998 A self-consistent model for the stress–strain behavior of shape-memory alloy polycrystals. *Acta Mater.* **46**, 5423–5433.

Otsuka, K. & Shimizu, K. 1974 Morphology and crystallography of thermoelastic Cu–Al–Ni martensite analyzed by the phenomenological theory. *Trans. Jpn Inst. Met.* **15**, 103–108.

Otsuka, K. & Shimizu, K. 1986 Pseudoplasticity and shape memory effects in alloys. *Int. Metall. Rev.* **31**, 93–114.

Shu, Y. & Bhattacharya, K. 1998 The influence of texture on the shape memory effect in polycrystals. *Acta Mater.* **46**, 5457–5473.

Smyshlyeav, V. P. & Willis, J. R. 1998 A 'non-local' variational approach to the elastic energy minimization of martensitic polycrystals. *Proc. R. Soc. Lond.* A **454**, 1573–1613.

Sun, Q. & Hwang, K. 1993*a* Micromechanics modelling for the constitutive behavior of polycrystalline shape memory alloys. I. Derivation of general relations. *J. Mech. Phys. Solids* **41**, 1–17.

Sun, Q. & Hwang, K. 1993*b* Micromechanics modelling for the constitutive behavior of polycrystalline shape memory alloys. II. Study of individual phenomena. *J. Mech. Phys. Solids* **41**, 19–33.

Thamburaja, P. & Anand, L. 2001 Polycrystalline shape-memory materials: effect of crystallographic texture. *J. Mech. Phys. Solids* **49**, 709–737.

Theil, H. & Van de Panne, C. 1960 Quadratic programming as an extension of classical quadratic maximization. *Mgmt Sci.* **7**, 1–20.

Wayman, C. M. 1964 *Introduction to the crystallography of martensitic transformations*. London: Macmillan.

Wechsler, M. S., Lieberman, D. S. & Read, T. A. 1953 On the theory of the formation of martensite. *Trans. AIME* **197**, 1503–1529.

Zhao, L., Willemse, P., Mulder, J. & Beyer, J. 1998 Texture development and transformation strain of a cold-rolled Ti50-Ni45-Cu5 alloy. *Scr. Mater.* **39**, 1317–1323.